THE ASTROPHYSICAL JOURNAL, 312:822–829, 1987 January 15

MICROWAVE OBSERVATIONS OF THE FLARE STARS UV CETI, AT MICROSCOPII, AND AU MICROSCOPII

M. R. KUNDU, P. D. JACKSON, S. M. WHITE, AND M. MELOZZI
Astronomy Program, University of Maryland
Received 1986 January 6; accepted 1986 July 7

ABSTRACT

We report on VLA observations of the red dwarf flare stars UV Cet, AT Mic, and AU Mic. All three stars flared during the observations. UV Cet exhibited a 10 mJy, 40% polarized flare at 20 cm, with no accompanying flare detected at 6 cm. The 6 cm quiescent emission was measured to be 2.8 mJy, higher than previously found. The primary star in the UV Cet system, L726-8A, showed a small, 100% polarized flare at 20 cm. Both components of the AT Mic system were found to be active and variable at both 6 and 20 cm. The peak emission levels were 10 mJy at 6 cm, and 7 mJy at 20 cm, in both cases from the south component of the system. AU Mic showed a 26 mJy, 90% polarized flare at 20 cm, with quiescent emission but no detectable flaring at 6 cm.

We discuss models for the quiescent microwave-emitting corona of UV Cet. The gravitational scale height in current models is similar to or larger than the height of the corona, which is a striking difference from the case of the solar corona, and confirms that magnetic structures are required to confine the radio-emitting corona. The role of precipitation into the chromosphere of the energetic particles in such a corona is explored. We show that for plausible parameters it may be the dominant energy loss mechanism.

Subject headings: polarization — stars: chromospheres — stars: flare — stars: radio radiation

I. INTRODUCTION

Red dwarf flare stars are of interest not only in their own right, but also because they aid us in understanding solar activity. Activity on red dwarf stars is driven by a convective layer, as on the Sun, and some flares (e.g., Kahler *et al.* 1982) can be understood as scaled-up replicas of solar flares. However, microwave observations of such stars have shown behavior not so readily explicable in solar terms (Gibson 1983; Gary 1985; Dulk 1985). Interest has focused on two aspects of the observations: the properties and source of microwave flares, and the variability and origin of quiescent emission. Here we report on flare star observations which encompass both these aspects. Red dwarf flares, unlike solar flares, are known to show both high brightness temperature and high polarization and are seldom correlated with optical flaring (Fisher and Gibson 1982). The quiescent microwave emission of the Sun would not be visible at the distance of any of the observed flare stars (Gary 1985). Thus flare stars show a range of behavior different from solar phenomena, and comparison will allow us to understand how differences in stellar structures lead to differing phenomena in the corona.

This paper describes the results of observations of three red dwarf flare star systems, UV Ceti, AT Mic and AU Mic, made in 1985 February and March. In § II the observations are described, and the results are presented in § III. Flaring was detected from all three systems, and quiescent emission from UV Cet and AU Mic. In § IV we discuss the results and relate them to earlier work. The flare parameters are calculated where appropriate. Quiescent microwave-emitting coronae are discussed in § V. One important aspect of these coronae is the power input from the lower layers of the stellar atmosphere required to maintain them. This may be deduced by considering the energy loss mechanisms which deplete the corona. We show that gravitational effects are less important in present models for the corona of UV Cet than they are on the Sun, and that as a consequence precipitation from the corona into the chromosphere may be the dominant loss mechanism. The results are summarized in § VI.

II. OBSERVATIONS

The observations were carried out on 1985 February 5–6 and March 22 using the Very Large Array of the National Radio Astronomy Observatory[1] near Socorro, New Mexico, in the "A" configuration (February) and the "AB" hybrid configuration (March) at 6 and 20 cm wavelengths. The normal observing mode was to make observations of 5 minutes duration at each frequency sequentially using the entire array. After each set of five such observations (20, 6, 20, 6, and 20 cm), a nearby calibrator was observed and the sequence then was repeated until the end of the observing time. This procedure gives the best sensitivity for studying quiescent emission and any slowly varying activity.

All observations were reduced using standard AIPS routines at the NRAO and were deconvolved using the CLEAN algorithms as implemented by Clark (1980).

III. OBSERVATIONAL RESULTS

a) UV Ceti

This system is a visual binary, L726-8AB, with separation of $\sim 2''$. The observations from 21:48 to 22:54 UT on February 6 had synthesized beamwidths of $1''.5$ (east-west) × $2''.5$ (north-south) at 20 cm and $0''.5 \times 0''.8$ at 6 cm, allowing resolution of both components. The source 0202−172 ($\alpha_{1950} = 02^{h}02^{m}34^{s}.515$, $\delta_{1950} = -17°15'39''.43$) was used as a calibrator for the observations of UV Cet.

On February 6, the flux density of UV Cet (726-8B) at 20 cm

[1] The National Radio Astronomy Observatory (NRAO) is operated by Associated Universities, Inc., under contract with the National Science Foundation.

was observed to increase from 1.7 ± 0.2 mJy to 3.2 mJy, and finally to ~10 mJy rather impulsively. Figure 1 shows the time variation of UV Cet's flux at 20 cm. From maps made in time steps of 1 minute during the impulsive rise phase (the last point in Fig. 1), we find that the flux increases from ~8 mJy to 12 mJy monotonically. At 6 cm UV Cet was essentially constant and unpolarized, with a time-averaged flux of 2.76 ± 0.08 mJy (errors are quoted as the rms noise). The primary star L726-8A was seen at 20 cm only during the first two intervals; it was below the limit of detection from the third interval through the impulsive rise phase. At 6 cm, the primary star shows only weakly on the time averaged map at a level of 0.34 ± 0.08 mJy.

The circular polarization of UV Cet at 20 cm during the first five intervals was not significant. However, in the sixth interval, that is, during the impulsive rise phase, the degree of polarization was ~40%. When broken into 1 minute intervals, the polarization varies from ~28% to 42%. The polarization of the primary at 20 cm during the first two intervals was almost 100%. The polarization of the primary at 6 cm was not significant.

The position of L726-8B was determined from the 6 cm data to be $\alpha_{1950} = 01^h36^m33\overset{s}{.}358 \pm 0\overset{s}{.}001$, $\delta_{1950} = -18°12'21\overset{''}{.}75 \pm 0\overset{''}{.}01$. The position of L726-8A was determined by combining the 20 cm and 6 cm positions and found to be $\alpha_{1950} = 01^h36^m33\overset{s}{.}281 \pm 0\overset{s}{.}004$, $\delta_{1950} = -18°12'23\overset{''}{.}59 \pm 0\overset{''}{.}08$, giving a position angle and separation of $30\overset{\circ}{.}8 \pm 1\overset{\circ}{.}8$ and $2\overset{''}{.}14 \pm 0\overset{''}{.}09$ respectively for this binary. The position errors for a single observation are assumed to be one-half the beamwidth divided by the signal-to-noise ratio. A discussion of the orbital motion of UV Cet from this and other radio positional data will be given by Jackson, Kundu, and White (1987).

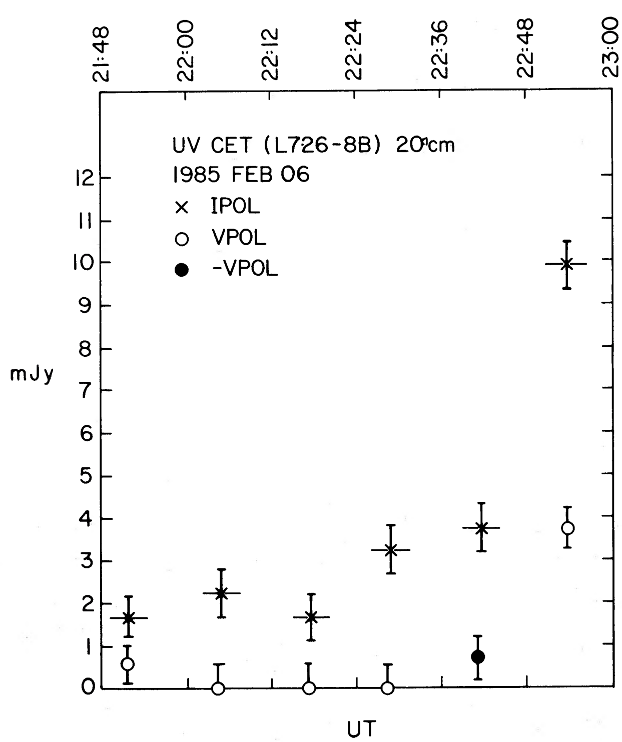

FIG. 1.—Variation of the total and circularly polarized flux density with time for UV Cet (L276-8B) at 1465 MHz on 1985 February 6. Vertical bars are 3 σ and horizontal bars show the range of UT spanned by each measurement.

b) *AT Microscopii*

This is another binary system ($3\overset{''}{.}5$ separation along a nearly north-south line), which was completely resolved in the observations of February 5 from 19:39 to 20:06 UT (synthesized beams of $1\overset{''}{.}3 \times 2\overset{''}{.}6$ at 20 cm and $0\overset{''}{.}4 \times 0\overset{''}{.}9$ at 6 cm). The observations of March 22 from 14:39 to 15:35 UT have beams of $4\overset{''}{.}1 \times 8\overset{''}{.}3$ at 20 cm and $1\overset{''}{.}3 \times 2\overset{''}{.}4$ at 6 cm; positional analysis (described by Gary, Linsky, and Dulk, 1982) was used to estimate the individual contributions to the total flux at 20 cm. The calibrator source for AT Mic was 2000−330 ($\alpha_{1950} = 20^h00^m13\overset{s}{.}021$, $\delta_{1950} = -33°00'12\overset{''}{.}5$).

On February 5, the N-component flux at 20 cm increased from 3.6 ± 0.3 mJy at 19:40 UT to 5.6 mJy at 19:53 and decreased again to 3.6 mJy at 20:05. This increase might be due to a gradual flare superposed on an already enhanced flux level. The S-component flux increased slightly from 4.9 mJy to 5.6 and then 5.7 mJy over the same intervals. Both components were essentially unpolarized at 20 cm. At 6 cm, the N-component flux was 3.6 ± 0.1 and 3.2 mJy at 19:46 and 20:00 UT respectively, while the S-component flux was 5.1 and 4.3 mJy. The N-component was unpolarized, while the S-component polarization at 6 cm was rather high, ~35%, at 20:00 but somewhat lower, ~17%, at 19:46. Figure 2 shows *I* and *V* maps at 20 cm and 6 cm for one 5 minute period. Both stars are evident in each *I* map; the *V* detections of the southern component in these maps are marginal.

On March 22, most (~90%) of the combined emission of 6.8 ± 0.2 mJy at 20 cm came from the S component, and no circular polarization was detected. The total period of observing was broken into five shorter intervals, showing marginally significant variations from ~6.2 mJy to ~7.1 mJy. At 6 cm, the map integrated over the entire period showed that the N component was much weaker (1.0 ± 0.1 mJy) than the S component (8.1 mJy). The S component was polarized (16%), while the N component was unpolarized. The maps produced over shorter time intervals (~5 minutes) showed only slight variations in the N-component flux while the S component underwent significant variations, from 9.6 ± 0.1 mJy at the beginning to 7.1 mJy toward the end of the observing period.

The measured 1950 positions for the S component at 6 cm were $\alpha = 20^h38^m44\overset{s}{.}396 \pm 0\overset{s}{.}001$, $\delta = -32°36'49\overset{''}{.}53 \pm 0\overset{''}{.}01$ on February 5 and $\alpha = 20^h38^m44\overset{s}{.}414 \pm 0\overset{s}{.}001$, $\delta = -32°36'49\overset{''}{.}58 \pm 0\overset{''}{.}01$ on March 22. For the N component, we obtained $\alpha = 20^h38^m44\overset{s}{.}466 \pm 0\overset{s}{.}001$, $\delta = -32°36'46\overset{''}{.}08 \pm 0\overset{''}{.}01$ on February 5 and $\alpha = 20^h38^m44\overset{s}{.}494 \pm 0\overset{s}{.}005$, $\delta = -32°36'46\overset{''}{.}18 \pm 0\overset{''}{.}12$ on March 22. The resulting position angles and separations are $14\overset{\circ}{.}5$ and $3\overset{''}{.}56$ on February 5 and $16\overset{\circ}{.}4$ and $3\overset{''}{.}55$ on March 22.

c) *AU Microscopii*

AU Mic and AT Mic form a physically associated pair, in that they have a common distance and proper motion, despite a separation by $1\overset{\circ}{.}5$ on the sky. Observations of AU Mic were made before and after the observations of AT Mic on March 22, from 13:13 to 14:38 and from 15:53 to 16:46 UT. The same calibrator, 2000−330, was used as for AT Mic. The beams were $3\overset{''}{.}3 \times 5\overset{''}{.}7$ at 20 cm and $1\overset{''}{.}2 \times 2\overset{''}{.}4$ at 6 cm. The measured position of the star at 6 cm was (1950) $\alpha = 20^h42^m04\overset{s}{.}558 \pm 0\overset{s}{.}004$, $\delta = -31°31'17\overset{''}{.}50 \pm 0\overset{''}{.}09$.

A major flare at 20 cm was in progress at the start of the first observing period, and Figure 3 shows the decay of this flare as measured over 13 time intervals of ~5 minutes each. Evi-

1987ApJ...312..822K

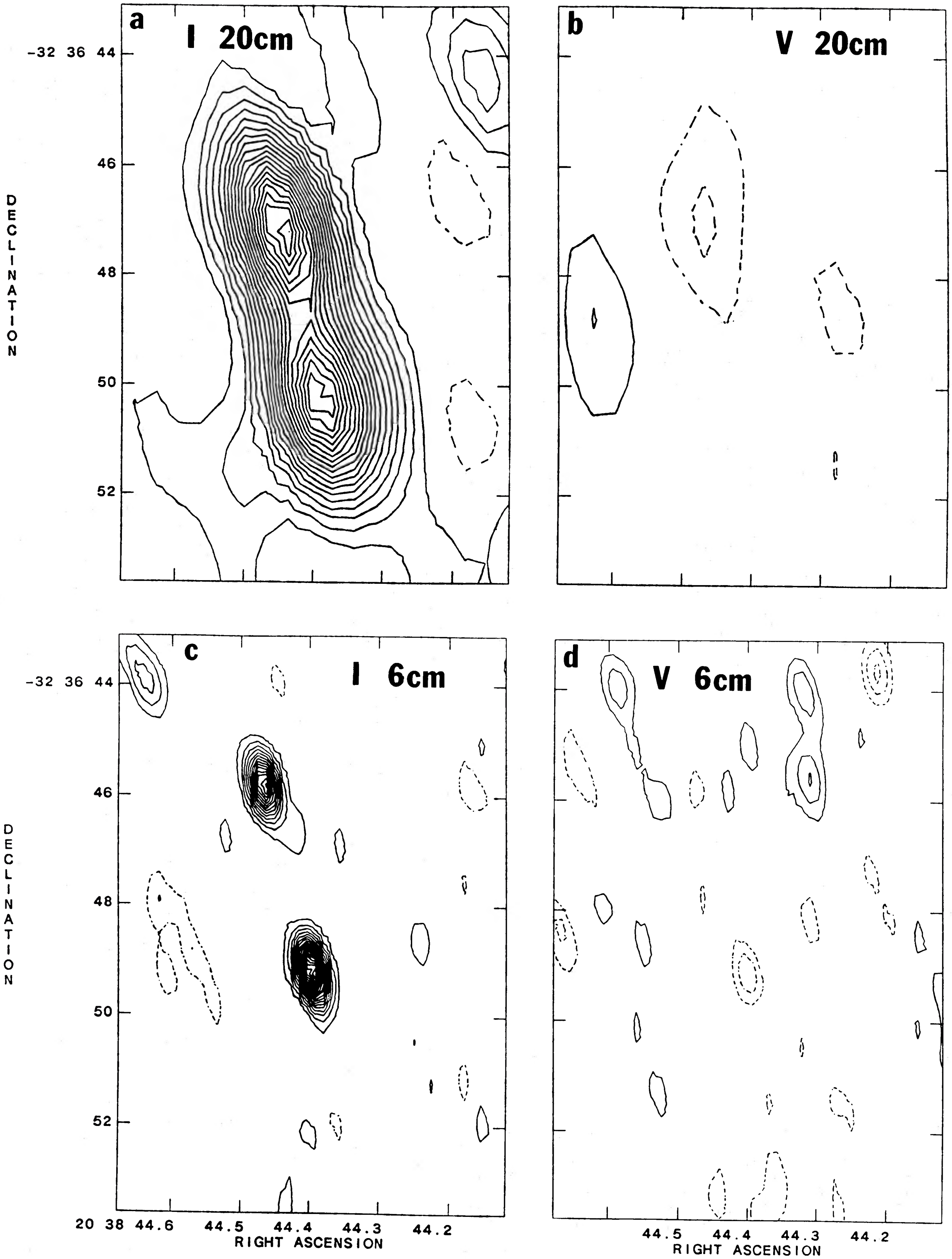

FIG. 2.—Maps of the AT Mic binary system during a 5 minute period when both stars were active. Both *I* and *V* maps at 20 cm (*a*)–(*b*) and 6 cm (*c*)–(*d*) are shown. Contour levels are multiples of 0.26 mJy in (*a*) and (*b*), of 0.23 mJy in (*c*), and of 0.22 mJy in (*d*). Note that due to the low altitude of this southern declination source during the observation the ionospheric refraction at 20 cm is severe and the positions of the stars are shifted relative to their 6 cm positions.

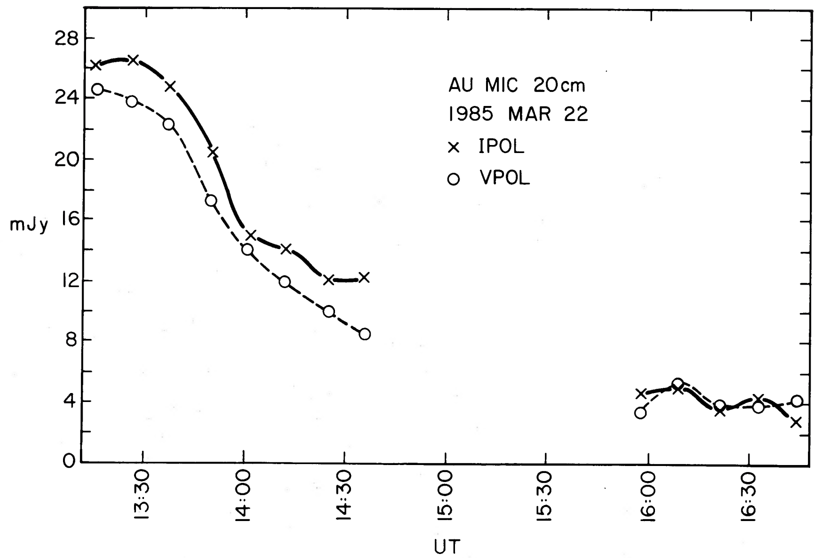

FIG. 3.—Variation of the total (IPOL) and polarized (VPOL) flux density with UT for AU Mic at 1490 MHz on 1985 March 22. Individual rms errors are typically ~0.25 mJy during the entire time interval and are not plotted.

dently, the observations started near the flare peak at 26 mJy and followed its decay to less than half this value 85 minutes later. After the break (for AT Mic), the flux was fairly steady at ~4 mJy. Figure 3 also shows the circularly polarized flux, V, and shows that the circular polarization was 70% to 90% or more throughout the observations. At 6 cm the flux remained constant, within the uncertainties of measurement, at $\sim 0.79 \pm 0.06$ mJy throughout, and this emission was not detectably polarized. The spectral index of the emission over the range 20 cm to 6 cm was thus extremely nonthermal, varying from steeper than -3.0 near the peak of the flare to steeper than -1.1 at the end of the flare.

In order to see how rapidly the emission might vary with frequency, separate maps were made at the frequencies 1465 MHz ("AC" correlators) and 1515 MHz ("BD" correlators). These maps showed that the emission at 1515 MHz was consistently ~10% weaker than at 1465 MHz, and this variation is consistent with a spectral index of ~ -3. However, such a steep spectral index does not continue down to meter-wave frequencies. Simultaneous observations of the field containing AU Mic and AT Mic were made at 57.5 MHz with the Clark Lake low-frequency synthesis radio telescope (Erickson, Mahoney, and Erb 1982). The upper limit for the 57.5 MHz flux density was ~3 Jy over a period of 1 hr, or 20 Jy over any 1 minute period.

IV. INTERPRETATION

At 6 cm the flux of UV Cet remained at 2.8 mJy for 1 hr. Deviations from this flux were below the noise level for each of the four 5 minute maps made during the 1 hr period. It is tempting, therefore, to regard 2.8 mJy as the quiescent emission level. However, this is about twice the values previously measured, 1.5 mJy in 1980 (Gary and Linsky 1981; Fisher and Gibson 1982) and 1.25 mJy in 1983 (Kundu and Shevgaonkar 1985). We conclude that either UV Cet was very slowly flaring at 6 cm, or that the quiescent emission level varies on a time scale of years. The latter is assumed to be the case for the discussion in § V.

The 2.8 mJy flux at 6 cm implies a coronal brightness temperature of $3.0 \times 10^8 (R/R_*)^{-2}$ K (for UV Cet we assume that $R_* = 0.24\ R_\odot$, $d = 2.7$ pc, and we use the formula $T_b = 2.0 \times 10^7\ S_{\rm mJy}\, d_{\rm pc}^2\, \nu_{\rm GHz}^{-2}\, (R/R_\odot)^{-2}$ K, which assumes that both polarizations contribute equally to the flux). Gary and Linsky (1981; see also Linsky and Gary 1983; Gary 1985) showed that the emission could not be thermal bremsstrahlung and argued that the flux could be explained by optically thick gyroresonance emission at a large harmonic ($s \approx 10$, $B \approx 200$ G) from an extended cooler corona ($R = 3\ R_*$, $T = 3 \times 10^7$ K). Alternatively the flux may be due to gyrosynchrotron emission by higher energy particles. Since the flux is unpolarized, we assume that the emission is optically thick. Using Figure 3 given by Dulk (1985), we deduce that optically thick gyrosynchrotron emission from a thermal distribution of electrons requires $NL > 10^{19}$ (N = number density, cm^{-3}; L = line-of-sight optical depth, cm) when the magnetic field B in the emitting region is 100 G; $NL > 10^{16}$ when $B = 200$ G; and $NL > 6 \times 10^{14}$ when $B = 300$ G. A characteristic scale length for emission at the sth harmonic is $B/s|\nabla B|$. In the model of Gary and Linsky (1981; $B_{\rm surface} = 2000$ G) this scale length is $\sim 2 \times 10^9$ cm at 100 G and 3×10^9 cm at 300 G. We adopt these as plausible values for L in a stellar corona ($R_* = 1.7 \times 10^{10}$ cm for UV Cet). Consequently, values of $N = 5 \times 10^5$ cm^{-3} at 100 G and 2×10^5 cm^{-3} at 300 G are implied. If the emission is due to optically thick gyrosynchrotron radiation by a nonthermal distribution of particles, we must estimate the spectral index δ of their energy distribution. Using the figures of Dulk (1985; Dulk and Marsh 1982), and assuming an angle of 40° between the line of sight and the magnetic field, we find that if $\delta = 3$, $NL > 10^{14}$ ($s = 4$, $B = 450$ G); if $\delta = 4$, $NL > 3 \times 10^{15}$ ($s = 5.5$, $B = 320$ G); and if $\delta = 5$, $NL > 1.5 \times 10^{17}$ ($s = 7$, $B = 260$ G). In this model a magnetic field of ~300 G in the emitting region again requires only a moderate density of hot particles, $N \approx 10^{5-6}$ cm^{-3}. These densities are well below the level at which the microwave-emitting particles could be detected in X-rays. These coronal models are discussed further in § V.

The 20 cm flare on UV Cet had a brightness temperature of $1.2 \times 10^{10} (R/R_*)^{-2}$ K. If $R = R_*$ and the emission is incoherent, it implies relativistic particles and hence synchrotron emission; however, it is then difficult to explain the absence of any detectable flare emission at the higher frequency, and the presence of significant circular polarization. The most curious feature of this flare is the sudden increase in polarization in the last minute of observation, from 22% (±3%) to 42% (±3%), while the total flux increased only slightly. If we assume that the flare occupies a large volume (e.g., $R = 2\ R_*$, $T = 3 \times 10^9$ K), the flux may be attributed to gyrosynchrotron emission which is just optically thick at 20 cm. However, in this model there is no simple way to increase the polarized flux density by an amount greater than the increase in the total flux density with a plausible change in the parameters of the gyrosynchrotron-emitting region. A more plausible interpretation is that a highly polarized source has switched on and is increasing its flux. Even this is difficult to achieve with conventional explanations, since a highly polarized source should be optically thin, yet the brightness temperature of the 5 mJy polarized flux is 1.5×10^9 K ($R = 2\ R_*$), again close to the synchrotron limit. If the highly polarized source is due to maser emission, then there is less difficulty in explaining the observation.

We note that these observations of the UV Cet system contain the second known example of closely spaced microwave flaring on both stars (Fisher and Gibson 1982). In addition, our observations are consistent with the pattern of previous observations of the system: flares on L726-8A tend to be highly polarized, with no accompanying quiescent emission (Fisher and Gibson 1982; Gary, Linsky, and Dulk 1982), while flares on UV Cet show a greater range of polarization and there is underlying quiescent emission at 6 cm.

We interpret the microwave flare on AU Mic to be further strong evidence for the role of maser action in radio stars (Holman, Eichler, and Kundu 1980; Gary, Linsky, and Dulk 1982; Lang *et al.* 1983; Dulk, Bastian, and Chanmugam 1983). With a distance of 8.85 pc and a radius $R_* = 0.5\ R_\odot$, a flux of 27 mJy at 20 cm implies a brightness temperature of 6.5×10^{10} $(R/R_*)^{-2}$. The high polarization, 90%, is not compatible with an incoherent emission mechanism at such a high brightness temperature, even if $R = 3\ R_*$. A narrow-band maser mechanism is compatible with the absence of any sign of flaring at 6 cm, where the flux implied a steady brightness temperature of $\sim 1.5 \times 10^8$ K. This is similar to the level found earlier by Cox and Gibson (1985) and strengthens the case for AU Mic being a quiescent emitter at 6 cm. The bandwidth of the 20 cm emission extends at least across the two observing frequencies of 1414 MHz and 1514 MHz, so it is not as narrowband as the isolated spike bursts observed on the Sun (relative bandwidth of less than 1%; Dröge 1977).

The observations of AT Mic confirm that both components of this binary system flare in microwaves. A flux of 6 mJy (seen from both stars) gives a brightness temperature of 4.0×10^{10} $(R/R_*)^{-2}$ K, with $d = 8.2$ pc and $R_* = 0.3\ R_\odot$ for dM4.5e stars. The 6 cm emission of 9 mJy on the S component gives $T_b = 5 \times 10^9\ (R/R_*)^{-2}$. Again, it is difficult to explain such high brightness temperatures by relying on the analogy with incoherent gyrosynchrotron emission known from solar microwave bursts, and coherent emission may be implied. We note that this observation appears to be unusual for red dwarf stars, in that the emission apparently due to flaring is not strongly polarized.

V. QUIESCENT STELLAR CORONAE

Despite some similarities between solar and stellar activity (see, e.g., Rodonò and Byrne 1983; Hjellming and Gibson 1985), the properties of the coronae of red dwarf stars based on models for quiescent emission must differ in important ways from the solar example. Here we explore some of the implications of these models. As is well known for both the Sun and other stars, X-ray and microwave observations reveal different components of the corona, with the X-rays showing cooler, denser, and deeper plasma than the microwaves (e.g., Gary 1985). We discuss only the (presumably) more extended microwave-emitting corona.

a) The Models

We discuss two models for the microwave-emitting quiescent corona. In the original model the emission was assumed to be due to thermal gyroresonance emission by a hot plasma (Gary and Linsky 1981; Gary 1985). We label this the "GR" model. In order to achieve sufficiently low temperature for gyroresonance emission to be valid, the corona must be extended, with $R = 3\ R_*$, $T = 3 \times 10^7$ K, and B = 200 G in the region emitting at 6 cm wavelength. The density of the 6 cm emitting layer in the model used by Gary and Linsky is $N \approx 2 \times 10^8$ cm^{-3}, and we assume that such a density is required to provide sufficient opacity.

In the second model, here called the "GS" model, the emission is assumed to be gyrosynchrotron emission by a hotter corona (Linsky and Gary 1983; Kundu and Shevgaonkar 1985). In the GS model $T_b = 2.7 \times 10^8$ K, $R = R_*$, $N = 10^{5-6}$ cm^{-3}, $B = 300$ G, and we assume that the height of the corona is less than $\approx 0.5\ R_*$.

In the following we first discuss the nature of the extended GR corona and then return to consider the hotter GS model.

b) Coronal Scale Height

The height of the corona must be determined by the magnetic structure for the following reason. In the GR model the ratio of the thermal energy of a typical ion at the surface of the star to its gravitational binding energy is

$$\frac{k_B T R_*}{G M_* m} \approx 1.8 , \qquad (1)$$

where we have assumed $m = 1.75\ m_p$ (i.e., proton mass), $R_* = 1.7 \times 10^{10}$ cm, $M_* = 0.1\ M_\odot$, and $T = 3 \times 10^7$ K (GR model). The corresponding scale height is $L_g = 1.8\ R_*$. At the emission height of 3 R_* in the GR model, the ratio given by equation (1) is a factor of 3 larger and L_g is an order of magnitude larger. By contrast, on the Sun $L_g = 0.04\ R_\odot$ at the surface. We argue that since the thermal energy of a typical particle in the corona of UV Cet dominates its gravitational binding energy, the quiet corona cannot be gravitationally bound and (as is widely believed) the trapping role of closed magnetic structures in the corona is crucial to its maintenance. For the same reason gravitation cannot be important in stratifying the corona, and the density gradient in the corona is expected to be small, i.e., the density at $R = 3\ R_*$ should not differ greatly from the coronal density just above the surface (for the purposes of illustration we assume this in the following discussion). These properties imply that, if the models based on quiescent microwave emission are appropriate, the quiet stellar corona is quite different from the solar corona where gravitational stratification is important. Density models based on the solar case are unlikely to apply to red dwarf stars.

c) *The Mean Free Path*

Another important coronal parameter is the Coulomb mean free path of an electron,

$$L_C = 10^4 T^2/N \text{ cm} \tag{2}$$

(Lang 1980). In the GR model ($N = 2 \times 10^8$ cm^{-3}, $T = 3 \times 10^7$ K) one finds $L_c = 4.5 \times 10^{10}$ cm $= 2.6\ R_*$. Since $R = 3\ R_*$, and the trapping magnetic loops in the GR corona have a length of typically 4–6 R_*; hence particles have several collisions in traveling from one end of the loop to the other.

d) *Energy Loss*

We now consider energy loss by the microwave-emitting electrons, which determines the rate at which energy must be supplied to the corona by the star. There are several pertinent time scales. One applies to the GS model if the hot particles coexist with a cooler denser plasma and is discussed later. A second loss time is given by radiative loss in a magnetic field. The lifetime of a particle in a 200 G field is 2.5 hr and in a 300 G field is 1 hr (Linsky and Gary 1983; Kundu and Shevgaonkar 1985). To these we add a third possible source of energy loss from the stellar corona, namely precipitation into the denser chromosphere. We are led to consider the role of precipitation by analogy with another well-studied example of a magnetically trapped particle population with little gravitational influence and a long mean free path, Earth's radiation belts. There, precipitation into the atmosphere is an important loss mechanism. Precipitation from coronal flux tubes into the chromosphere is known to be important during solar flares, and we now argue that the parameters of the above models make it important for quiescent stellar coronae also.

e) *Precipitation*

Why should precipitation be more important for flare stars than for the Sun? Precipitation occurs if the particle population in the corona is not in pressure balance with the lower atmosphere. In the quiet-Sun corona the mean free path is shorter than the scale height in the lower atmosphere, such that pressure balance can be maintained in a stratified atmosphere. Precipitation there is only relevant for magnetically confined hot plasma which has a mean free path longer than relevant scale heights, such as occurs through heating by a solar flare. In the GR model the mean free path is 2.6 R_*, and relevant gradient scale lengths cannot be any shorter than this. We argue that if there is pressure balance in the GR model for the UV Cet corona, then the gradient scale length would have to be several mean free paths thick, which is greater than the assumed height of the corona. Thus it seems unlikely that a stratified atmosphere can be attained with pressure balance, and precipitation concepts will be valid in the GR model also.

In the absence of scattering, magnetically trapped particles have loss cone velocity distributions (i.e., an absence of particles with small pitch angles). Scattering tends to fill the loss cones and cause precipitation (e.g., see Schulz and Lanzerotti 1974; Lyons and Williams 1984). In Earth's radiation belts, where the plasma frequency ω_p exceeds the gyrofrequency Ω, whistler waves are excited by the loss cone anisotropy and cause scattering (Kennel and Petschek 1966).

There are two important limits for precipitation of magnetically trapped particles. In the "weak diffusion" limit, particles are not scattered (on average) in one transit of the flux loop and the loss cone is mostly empty. In the "strong diffusion" limit, the mean free path for scattering is short. Scattering then isotropizes the velocity distribution, and the loss cones are filled. As noted above, in the GR model the mean free path is shorter than the length of the flux tube, and a particle typically undergoes two or three collisions in traversing a flux tube. Thus in the GR model the loss cones should be filled just by Coulomb scattering. Since the loss cone is continually emptied at the chromosphere, the particle lifetime is shortest in the strong diffusion limit, and only in this limit (approximately valid here) is precipitation likely to be important in determining the energy balance of stellar coronae. The lifetime of a particle in this limit is (Kennel 1969)

$$\tau_p = \frac{\tau_0}{2.2 \sin^2 \alpha_{LC}} , \tag{3}$$

where $\tau_0 = 2L/v$ is the particle bounce period (L is the length of a field line) and α_{LC} is the half-angle of the loss cone at the top of the corona where $B = B_0$ is minimum, i.e., $\sin^2 \alpha_{LC} = B_0/B_{\text{surface}}$. In the GR model ($B_0 = 200$ G, $B_{\text{surface}} = 2000$ G, $L = 4\ R_*$, $T = 3 \times 10^7$ K), we find

$$\tau_p = 350 \text{ s} .$$

This is much shorter than the radiative loss time. If τ_p determines the loss time scale, the rate of energy replacement in the GR model is of the order of 10^{30} ergs s^{-1} (assuming a filling factor for the corona equivalent to the filling factor of the quiescent emission). This is exceedingly high: it is two orders of magnitude greater than the X-ray or visual luminosities, whereas on the Sun the coronal heating rate ($< 10^{28}$ ergs s^{-1}) is many orders of magnitude below the total luminosity ($\sim 10^{33}$ ergs s^{-1}).

f) *The Gyrosynchrotron Model*

Due to the different parameters of the GS model ($R = R_*$, $T = 3 \times 10^8$, $N = 10^6$ cm^{-3}, $B = 300$ G), the nature of the corona is somewhat different from the GR model. First, the coronal scale height is $\sim 20\ R_*$, and the arguments regarding gravitational stratification apply even more strongly than in the GR case. Second, the mean free path is much longer: in the GS model, $L_c = 7 \times 10^{14}$ cm $= 4 \times 10^4\ R_*$. Even if the hot microwave-emitting plasma is embedded in a cooler plasma at 10^8 cm^{-3} (Linsky and Gary 1983), the collision length is 10^{13} cm. Thus for the hot particles collisions can only be important on time scales of several hundred seconds, and there can be no pressure balance between the hot particles and the lower atmosphere (in the absence of magnetic effects). The concept of precipitation is certainly valid.

In the GS model for the corona of UV Cet, Coulomb scattering cannot play any role in filling the loss cones of the velocity distribution, as it did in the GR case. However, in this case, as in Earth's magnetosphere, wave scattering may be important. For the parameters chosen ($B = 300$ G, $N = 10^6$ or 10^8 cm^{-3}), we have $\omega_p \ll \Omega$ in the corona. Velocity distributions with loss cone features in such a plasma are unstable to the generation of x-mode waves via electron cyclotron maser action (Wu and Lee 1979). Melrose and Dulk (1984) applied this idea to solar flares and showed that wave scattering may be important in maintaining precipitation in that context. Saturation of the maser occurs locally when the wave level is sufficiently high for scattering to isotropize the velocity distribution there. This is exactly the process which interests us. However, this form of saturation occurs briefly at a certain point and then ceases: it need not lead to strong diffusion occurring throughout the flux tube, which is required for maximum particle loss. Further, local saturation is not necessary for strong diffusion to be valid. All that is required is that the condition

$$D\tau_0 > 1$$

be satisfied, where D is the relevant pitch-angle scattering coefficient. We have calculated an approximate value for D by assuming that scattering is due to cold plasma x-mode waves with a brightness temperature of T_x, frequency just exceeding the cold plasma x-mode cutoff, and wave vector angles θ (between the wave vector and the magnetic field) which are close to 90°. These are the conditions favored by loss cone maser emission when $\omega_p \ll \Omega$. The assumption of cold plasma wave dispersion is probably not strictly valid if $T = 2.7 \times 10^8$ K (see, e.g., Winglee 1985, and references therein) but should be satisfactory as an approximation. Following the related calculation in, e.g., Melrose and White (1980), we find that

$$D = \frac{e^2}{4}\frac{\omega_p^2}{\Omega^2}\frac{1}{m^2 v^3}\int dkkT_x(k)\left[\frac{1}{(1-n^2)} + \frac{\Omega^2}{\omega_p^2}\cos^2\theta\right]^2 , \quad (4)$$

where n is the refractive index, m the electron mass, and v the thermal speed. Choosing the value $n^2 = 1/2$ as representative, setting $\cos^2\theta = 0$, and assuming that the wave vector spectrum of the amplified waves has a relative width $\Delta k/k$, the diffusion coefficient takes the value

$$D = 1.4 \times 10^{-11}\ T_x \Delta k/k .$$

In the GS model $\tau_0 \approx 2$ s; then if $\Delta k/k > 0.01$, an average brightness temperature of $\sim 10^{13}$ K throughout the flux tube would be sufficient to cause strong diffusion (note that we assume that the fundamental x-mode waves cannot escape from the corona, and so this maser radiation would not be observed. The quiescent emission is at higher harmonics of the gyrofrequency and can escape.) This brightness temperature is well below the levels typically estimated to be necessary for local saturation ($\sim 10^{20}$ K; e.g., Melrose and Dulk 1984). However, strong diffusion as envisaged here still fills the loss cones and turns off the maser, preventing wave growth and so turning off the scattering. We do not expect that this process will occur uniformly throughout the corona. Thus we assume that at any given time strong diffusion is only occurring in some fraction η of the volume of the corona, and that the particle lifetime is correspondingly increased by a factor of $\sim \eta^{-1}$. Alternatively, it seems plausible that in a quiescent corona a marginally steady state is established, in which the scattering is not strong enough to fill the loss cones and the resulting maser growth rate is sufficient to maintain the wave level at the marginally steady level. In this case the particle lifetime is again $\eta^{-1}\tau_p$, where now η is the filling fraction of the loss cone.

In the GS model $\tau_p \approx 10$ s, and we require $\eta > 0.3\%$ (with a radiative loss time of 4.3×10^2 s) for precipitation to dominate over radiative loss. The radiative loss model requires a coronal heating rate of $\sim 4 \times 10^{26}$ ergs s^{-1} if the energy distribution is thermal (assuming a coronal height of 0.5 R_*); precipitation implies a heating rate of $1.8 \times 10^{29}\ \eta$ ergs s^{-1}. The energy distribution should be thermal if the loss time ($10/\eta$ s) is much longer than the thermalization time (several times the time between collisions, or ~ 50 s); if η is close to one the distribution is nonthermal, and depending on the energy spectrum the required heating rate may be larger. As mentioned above, there is another energy loss mechanism for the GS model if the hot plasma is embedded in a cooler denser plasma. The two components come to thermal equilibrium via collisions, quenching the microwave emission, in ~ 240 s with $T = 2.7 \times 10^8$ K and $N = 10^8$ cm^{-3} (Linsky and Gary 1983). This corresponds to a coronal heating rate of $\sim 5 \times 10^{27}$ ergs s^{-1}, which exceeds the radiative loss rate.

g) Consequences of Precipitation

In this section we have pursued the consequences of stellar coronal models based on the quiescent microwave emission. There are a number of other aspects of the precipitation model which we will briefly mention here, but whose detailed investigation is beyond the aims of this discussion. The energy of the precipitating particles must somehow be lost by the lower atmosphere. Cram (1982) discusses a similar problem: from his results we conclude that radiation by the chromospheric and transition region lines can account for at most $\sim 10^{28}$ ergs s^{-1}. This is adequate for the GS model provided that $\eta < 5\%$, but too low for the GR model. The relationship between precipitation and the quiescent X-ray flux needs to be investigated. During solar flares, precipitating energetic electrons produce hard X-ray emission, and so we might expect that at least part of the stellar X-ray flux results from this mechanism. However, the spectrum of bremsstrahlung from electrons with the energies derived for the microwave-emitting particles seems to disagree with the observed spectrum. If the precipitating particles are not directly responsible for the X-rays, then both lead to heating of the chromosphere and the transition region. Cram (1982) considered the consequences of heating by the X-ray flux. The particle energy will tend to be dumped in higher layers of the amosphere than the X-ray flux, since the cross section for scattering of charged particles (due to Coulomb scattering in a plasma and to ionization interactions in a neutral gas) is higher than that for scattering of X-rays (Thompson scattering in a plasma, Rayleigh scattering in a neutral gas). Thus the two energy sources may lead to different ratios of chromospheric and transition region emission.

In conclusion, current models for microwave-emitting quiescent stellar coronae display important differences from the solar case. The concept of precipitation, borrowed from Earth's radiation belts, may be important in determining the energy loss rate in these models. If so, the heating rate required for the extended gyroresonance-emitting coronal model is unacceptably large and appears to rule out this model. The heating rate for the gyrosynchrotron-emitting model corona is smaller.

VI. CONCLUSION

The most powerful microwave emissions observed on the Sun are the impulsive bursts associated with solar flares, with brightness temperatures up to 10^{10} K (Kundu 1982). At these brightness temperatures the accompanying polarization can reach at most 40%; such bursts usually last less than 10 minutes and may be attributed to nonthermal gyrosynchrotron emission by energetic particles accelerated in the flare. Longer duration emissions have lower brightness temperatures. The highest brightness temperature bursts observed at microwave frequencies are the spike bursts (Dröge 1977; Slottje 1978), which are narrow-band and very brief (< 10 ms).

The microwave observations of red dwarf flare stars reported here confirm that these stars are more active in microwaves than the Sun, and that the observed flares cannot be easily explained using the solar analogy. In particular, the long, highly polarized, high brightness temperature flare on AU Mic cannot be explained by known incoherent emission mechanisms, and a coherent emission mechanism is required.

Quiescent emission at 6 cm from UV Cet has again been detected, this time at a level (2.8 mJy) approximately twice the flux measured in previous observations. This indicates that the quiescent flux may be variable at least on the time scale of years and opens the possibility that cyclical behavior may be detected by further monitoring.

We have investigated the thermal gyroresonance and nonthermal gyrosynchrotron models for the quiescent emission of UV Cet. An important difference between the solar corona and UV Cet is that the gravitational scale height on UV Cet in these models is larger than the stellar radius, and hence magnetic confinement of the coronal plasma must be even more important than it is on the Sun. For this reason precipitation of the coronal particles into the chromosphere may be the dominant energy loss mechanism for the corona of UV Cet and will determine the coronal heating rate needed to maintain quiescent emission in these models. The large heating rate for the extended gyroresonance-emitting corona appears to rule out this model. Precipitation in the gyrosynchrotron-emitting model could be related to the X-ray emission of the red-dwarf stars.

This research was primarily supported by a basic research grant from the University of Maryland. Partial support was also received from NSF grant ATM 84-15388 and NASA grant NGR 21-002-199. We thank the referee for his careful reading of the manuscript and his thoughtful comments. A number of these comments have been incorporated in the text. We also thank E. Schmahl for his comments on the manuscript, and S. M. W. would like to thank D. Zarro for a helpful discussion.

REFERENCES

Clark, B. G. 1980, *Astr. Ap.*, **89**, 377.
Coleman, G. D., and Worden, S. P. 1976, *Ap. J.*, **205**, 47.
Cox, J. J., and Gibson, D. M. 1985, in *Radio Stars*, ed. R. M. Hjellming and D. M. Gibson (Dordrecht: Reidel), 233.
Cram, L. E. 1982, *Ap. J.*, 1982, **253**, 768.
Dröge, F. 1977, *Astr. Ap.*, **57**, 285.
Dulk, G. A. 1985, *Ann. Rev. Astr. Ap.*, **23**, 169.
Dulk, G. A., Bastian, T. S., and Chanmugam, G. 1983, *Ap. J.*, **273**, 245.
Dulk, G. A., and Marsh, K. A. 1982, *Ap. J.*, **259**, 350.
Erickson, W. C., Mahoney, M. J., and Erb, K. 1982, *Ap. J. Suppl.*, **50**, 403.
Fisher, P. L., and Gibson, D. M. 1982, in *Second Cambridge Workshop in Cool Stars*, vol. **2**, ed. M. S. Giampapa and L. Golub (Cambridge: Smithsonian Ap. Obs.), p. 109.
Gary, D. E. 1985, in *Radio Stars*, ed. R. M. Hjellming and D. M. Gibson (Dordrecht: Reidel), p. 185.
Gary, D. E., and Linsky, J. L. 1981, *Ap. J.*, **250**, 284.
Gary, D. E., Linsky, J. L., and Dulk, G. A. 1982, *Ap. J.* (*Letters*), **263**, L79.
Gibson, D. M. 1983, in *IAU Colloquium 71, Activity in Red Dwarf Stars*, ed. P. Byrne, and M. Rodonò (Dordrecht: Reidel), p. 273.
Golub, L. 1983, in *IAU Colloquium 71, Activity in Red Dwarf Stars*, ed. P. Byrne, and M. Rodonò (Dordrecht: Reidel), p. 83.
Hjellming, R. M., and Gibson, D. M. ed. 1985, *Radio Stars* (Dordrecht: Reidel).
Holman, G. D., Eichler, D., and Kundu, M. R. 1980, in *IAU Symposium 86, Radio Physics of the Sun*, ed. M. R. Kundu and T. E. Gergely (Dordrecht: Reidel), p. 457.
Jackson, P. D., Kundu, M. R., and White, S. M. 1987, in preparation.
Kahler, S., *et al.* 1982, *Ap. J.*, **252**, 239.
Kennel, C. F. 1969, *Rev. Geophys.*, **1**, 379.
Kennel, C. F., and Petschek, H. E. 1966, *J. Geophys. Res.*, **81**, 2275.
Kundu, M. 1982, *Rept. Progr. Phys.*, **45**, 1435.
Kundu, M. R., and Shevgaonkar, R. K. 1985, *Ap. J.*, **297**, 644.
Lang, K. R. 1980, *Astrophysical Formulae*, (New York: Springer Verlag), p. 56.
Lang, K. R., Bookbinder, J., Golub, L., and Davis, M. M. 1983, *Ap. J.* (*Letters*), **272**, L15.
Linsky, J. L., and Gary, D. E. 1983, *Ap. J.*, **274**, 776.
Lyons, L. R., and Williams, D. J. 1984, *Quantitative Aspects of Magnetospheric Physics* (Dordrecht: Reidel).
Melrose, D. B., and Dulk, G. A. 1982, *Ap. J.*, **259**, 844.
———. 1984, *Ap. J.*, **282**, 308.
Melrose, D. B., and White, S. M. 1980, *J. Geophys. Res.*, **85**, 3442.
Rodonò, M., and Bryne, P., ed. 1983, *Activity in Red Dwarf Stars* (Dordrecht: Reidel).
Schulz, M., and Lanzerotti, L. J. 1974, *Particle Diffusion in the Radiation Belts* (New York: Springer).
Slottje, C. 1978, *Nature*, **275**, 520.
Vaiana, G. S., *et al.* 1981, *Ap. J.*, **245**, 163.
Winglee, R. M. 1985, *Ap. J.*, **291**, 160.
Wu, C. S., and Lee, L. C. 1979, *Ap. J.*, **230**, 621.

P. D. JACKSON, M. R. KUNDU, and S. M. WHITE: Astronomy Program, University of Maryland, College Park, MD 20742

M. MELOZZI: via Caracciolo 12, 50100 Firenze, Italy